GRUPPO NAZIONALE DI GEOFISICA DELLA TERRA SOLIDA
33° Convegno Nazionale Bologna

The Deep Structure of the Larderello-Travale Geothermal Field (Italy) from Integrated, Passive Seismic Investigations.

Gilberto Saccorotti [(1)], Davide Piccinini [(1)], Maria Zupo [(1,2)], Francesco Mazzarini [(1)], Lena Cauchie [(1,3)], Claudio Chiarabba [(1)], Nicola Piana Agostinetti [(1,4)], Matteo Bagagli [(1)]

(1) Istituto Nazionale di Geofisica e Vulcanologia, Italy
(2) Università degli Studi di Bologna
(3) University College of Dublin – School of Geological Sciences, Dublin, Ireland.
(4) Dublin Institute for Advanced Studies, Geophysics Section, Dublin, Ireland

INGV

The Larderello-Travale geothermal field (LTGF; Italy)

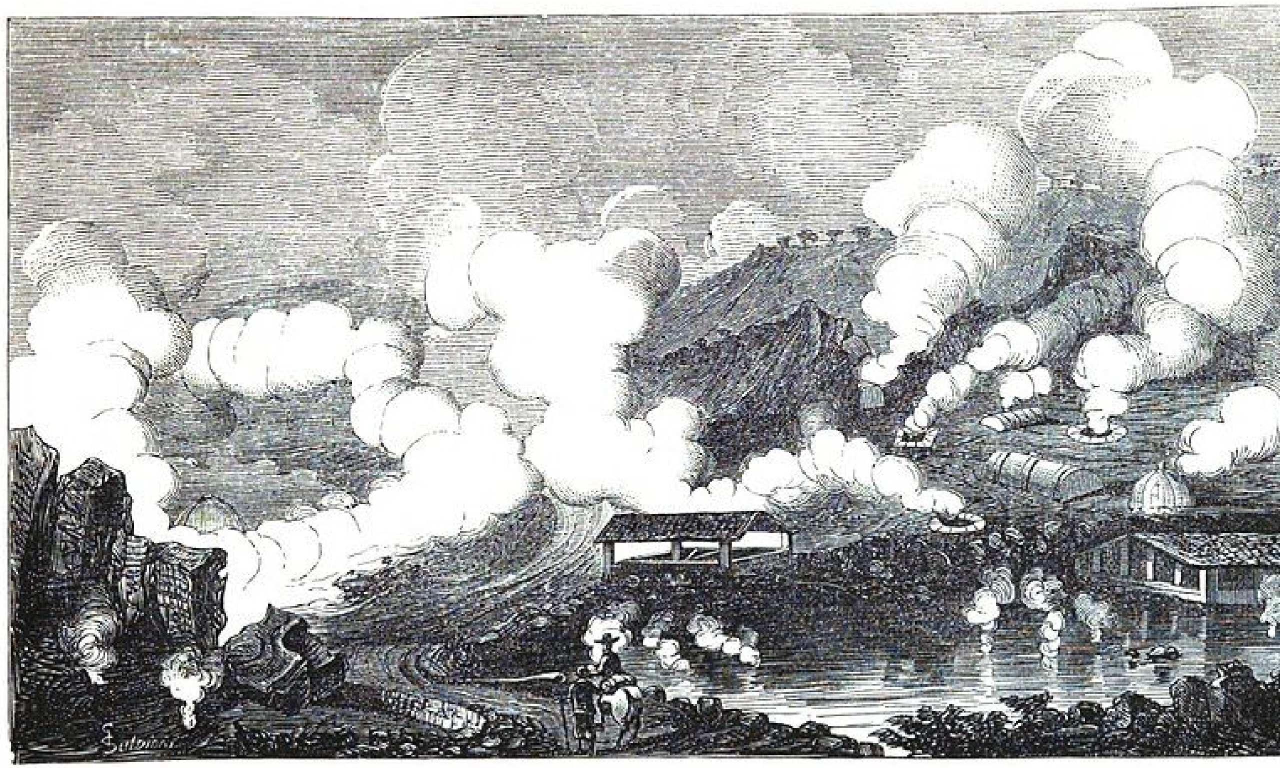

Geothermal exploitation at LTGF started in 1905; it is the world's oldest geothermal production plant.

Actual production rate amounts to **4800 GWh / yr**, which is ~ 10% of the world's geothermal energy budget.

BASIC GEOLOGY

Oligocene–Middle Miocene Apenninic tectonic pile of nappes.

Adriatic paleo-margin (Tuscan metamorphic units, Tuscan wedge), Palaeozoic to Early Miocene.

Pliocene & Quaternary Granitic intrusions

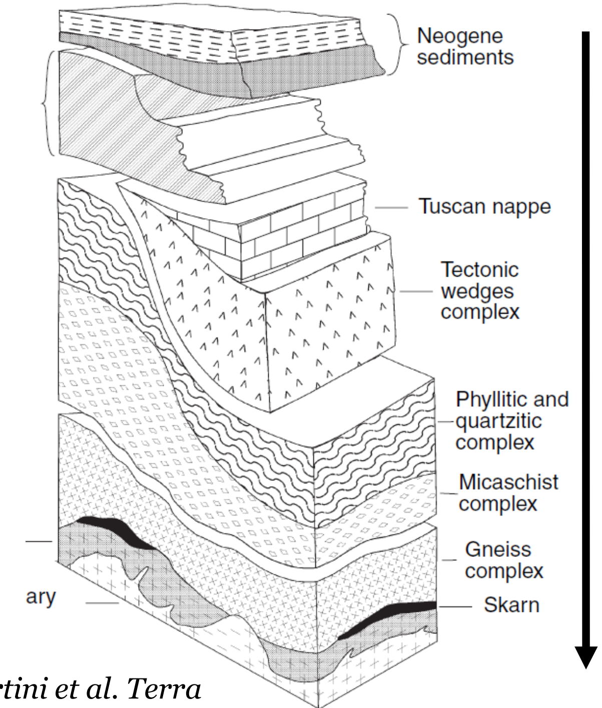

G. Bertini et al. Terra Nova, Vol 18, No. 3, 163–169

EXPLOITATION

Till early '80s: Shallow Carbonate reservoir
T ~ 250°, Z < 1000 m

More recently: Super-heated (T~350°) steam reservoirs at Z > 3500-4000m within the metamorphic and intrusive units.

The 2 main seismic horizons

K marker: A deep reflector entirely reconstructed by seismic interpretation. Various hypotheses on its origin: (brittle/ductile transition zone, supercritical fluids, metamorphic aureole caused by a **very recent** intrusion).

H marker: Contact metamorphic aureole associated with the shallower Pliocene granites. The higher fracturing and permeability make this marker **a valuable target for exploitation**.

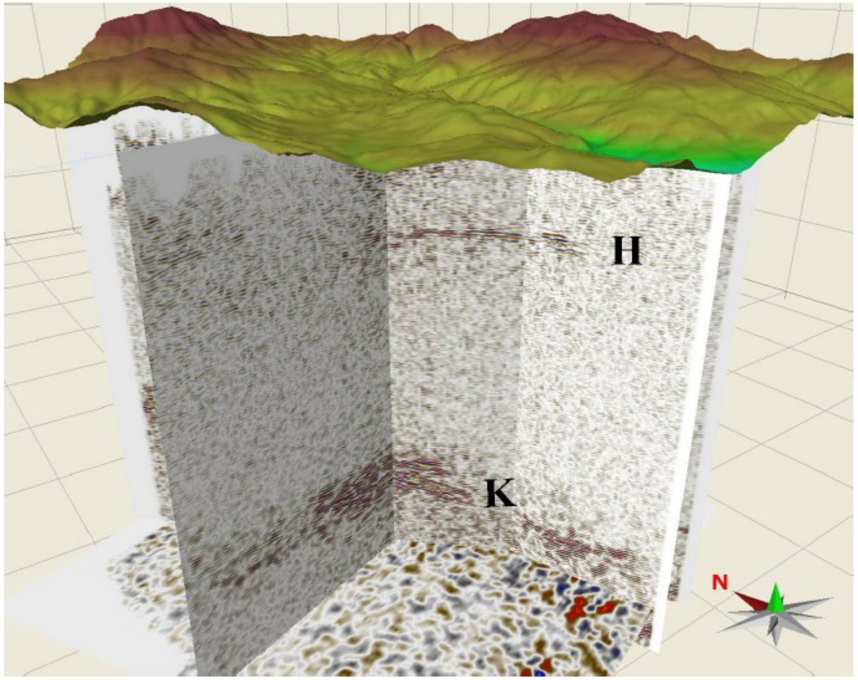

Casini et al., Proceedings World Geothermal Congress 2010

The GAPSS Experiment

12-20 stand-alone seismic stations
Sensors @ 5s, 30s, 120s
Aperture: ~ 50 km
Spacing: ~ 5-10 km

GOALS:
Velocity and Q L.E.T
Anisotropy Studies
Shear-wave velocity profiles
Ambient Noise Velocity Tomography
Induced Seismicity (criteria for discernment of)

BEGIN: May, 2012
END: October, 2013

GAPSS Data Set

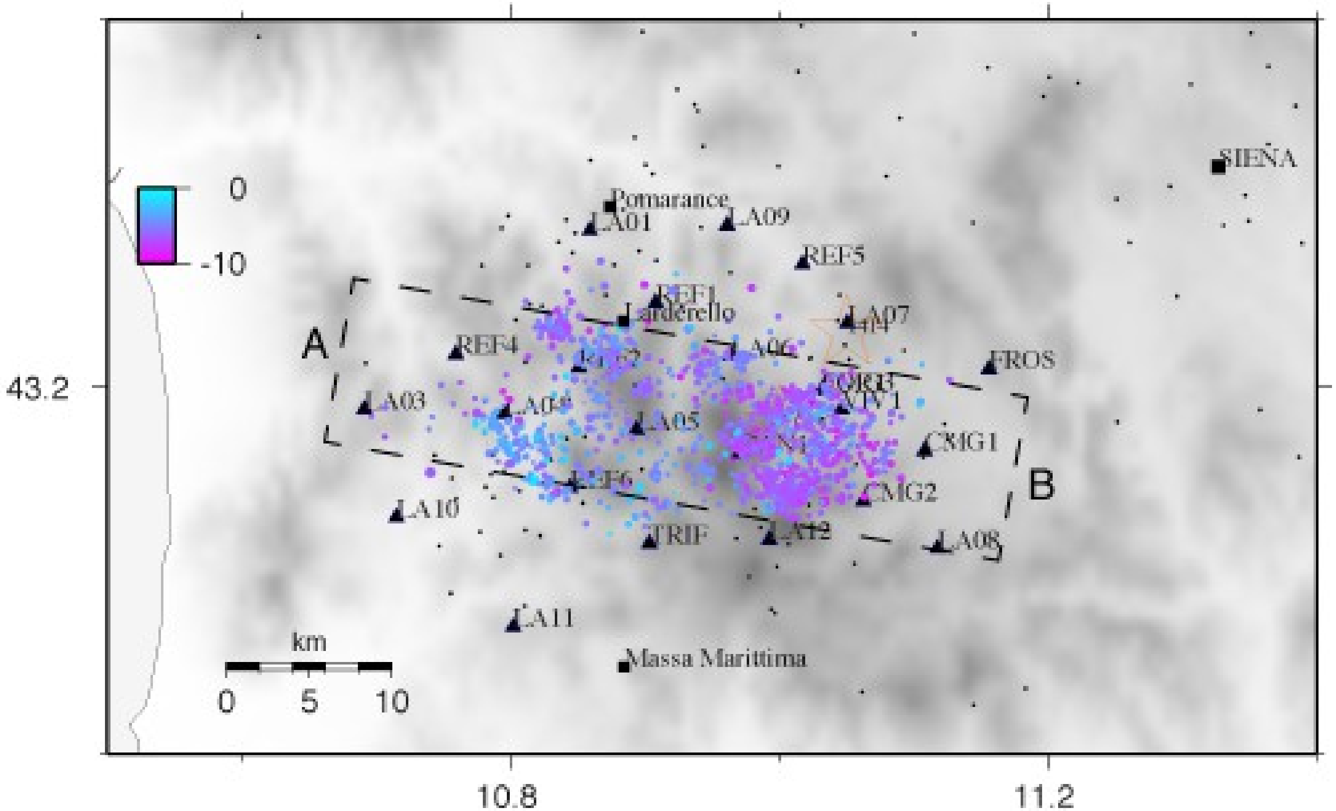

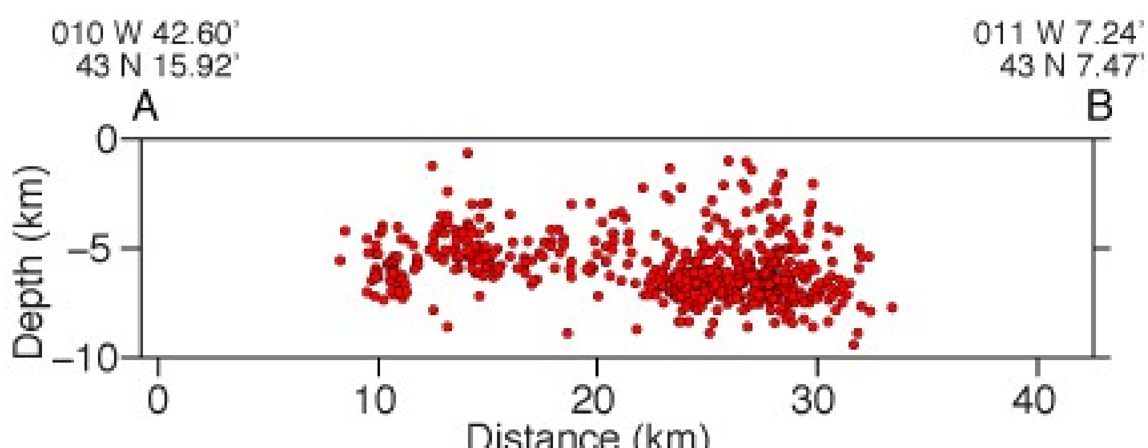

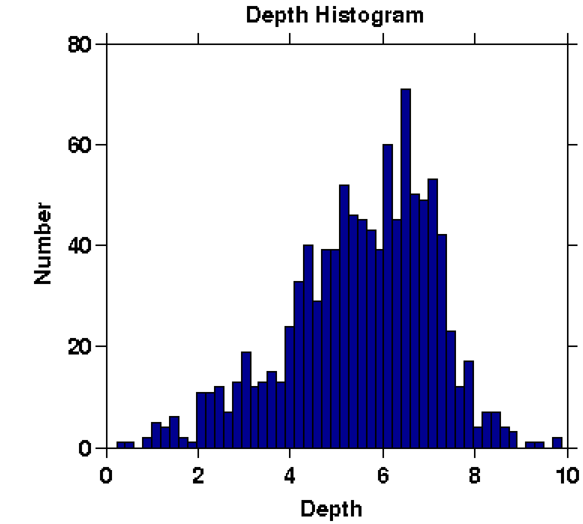

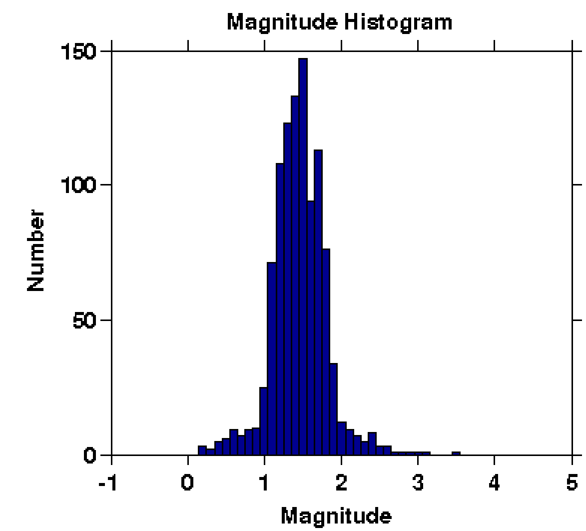

Mmax:	**3.5**
Mc:	**1.5**
B-value:	**1.4**
Rate:	**up to 50 eq/day**

Shear-Wave-Splitting: fast S-wave polarisation directions

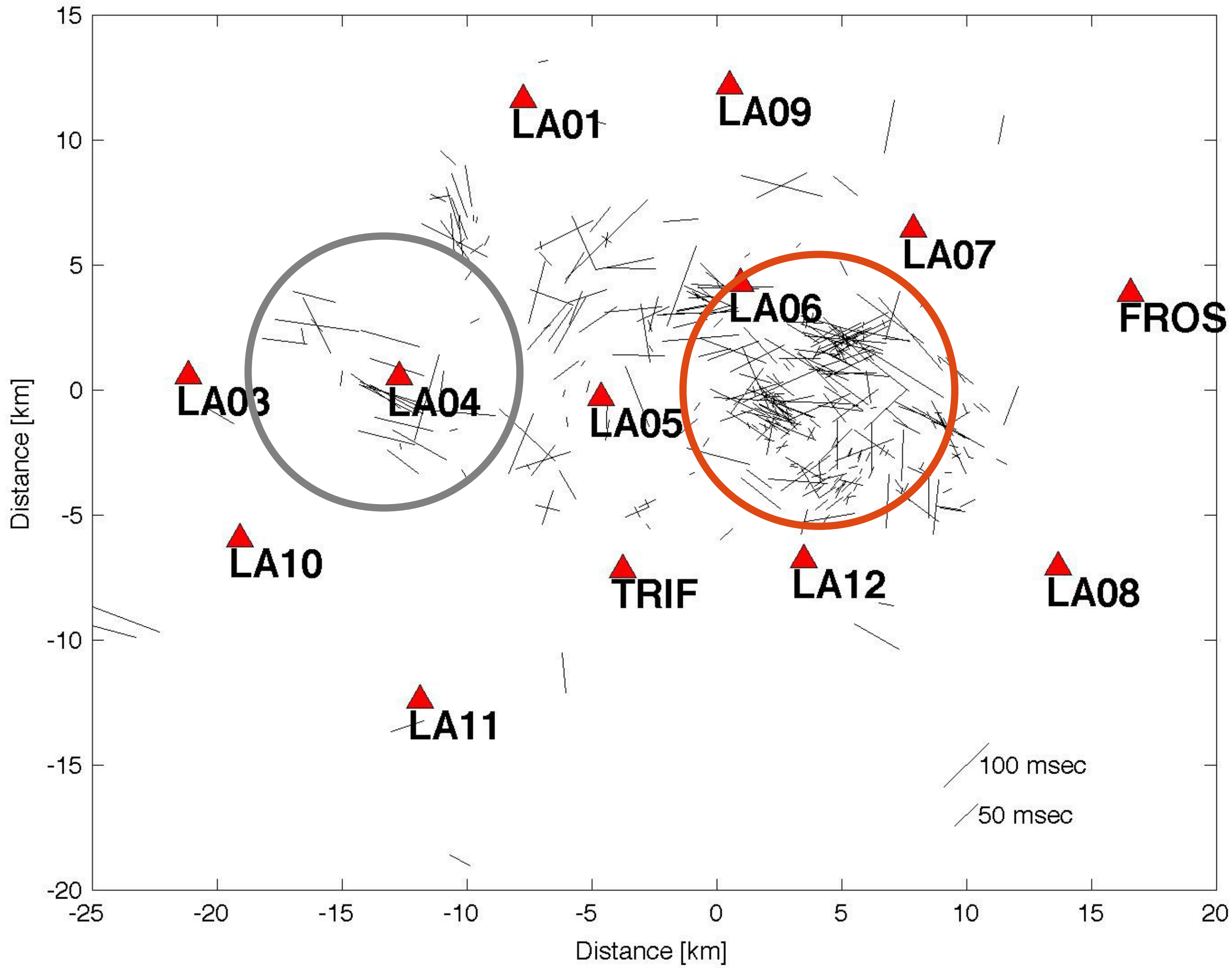

The polarisation directions of the fast S-wave within the geothermal field are much more scattered than in its peripheral parts

Shear-Wave-Splitting: S-wave delay times

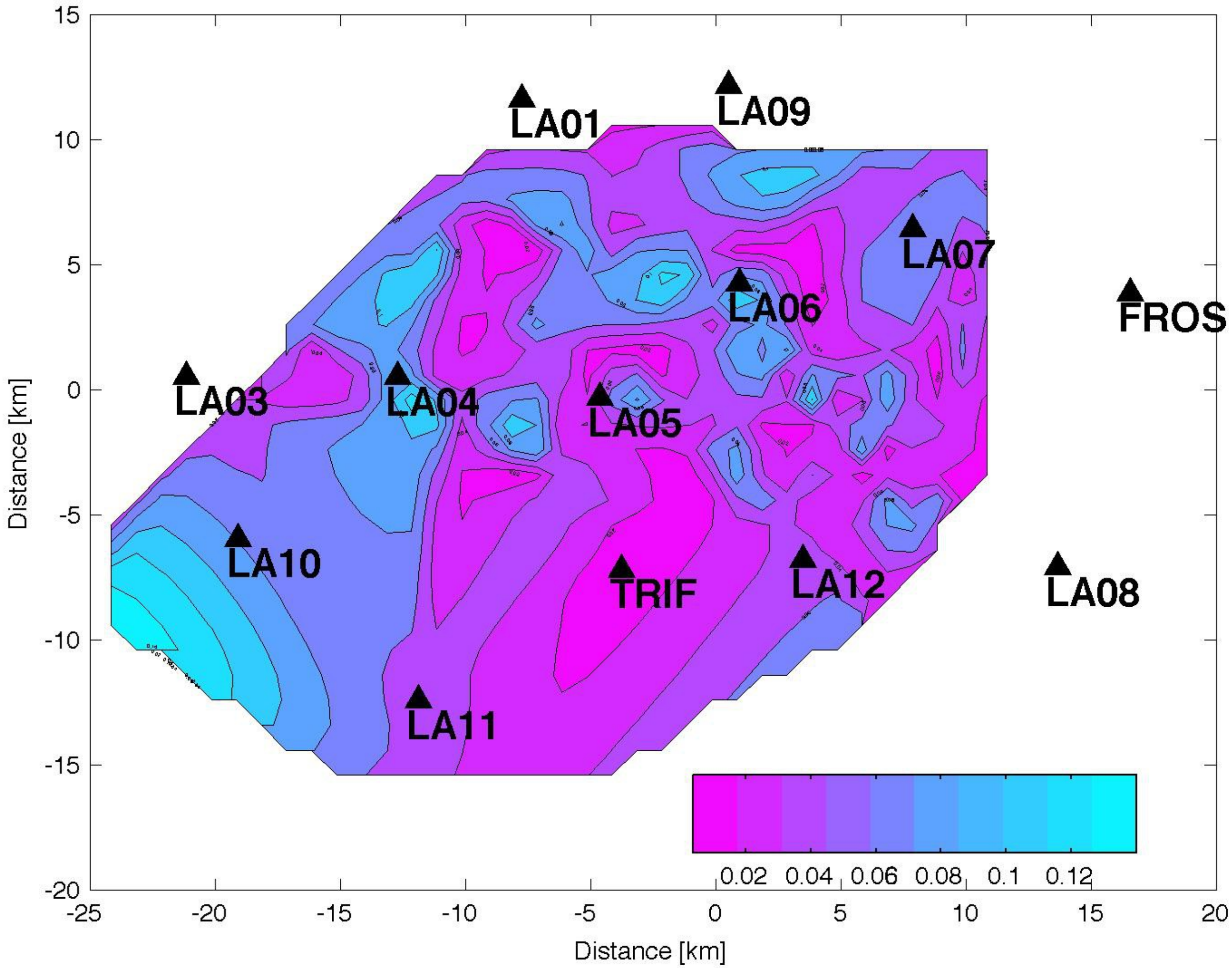

The same holds for the delay times, which are greater within the productive areas.

Depth of anisotropic layers from Dt inversion

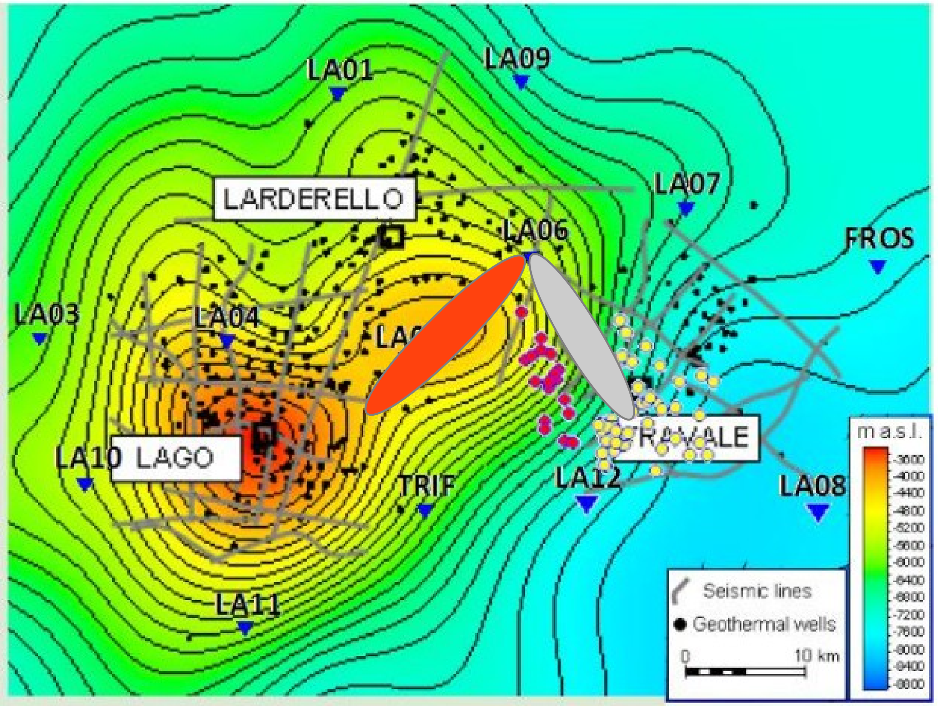

S-wave delay times are inverted for the depth of anisotropic layers, for a medium with cylindrical simmetry. Results suggests that most of the anisotropy is related to the K-horizon.

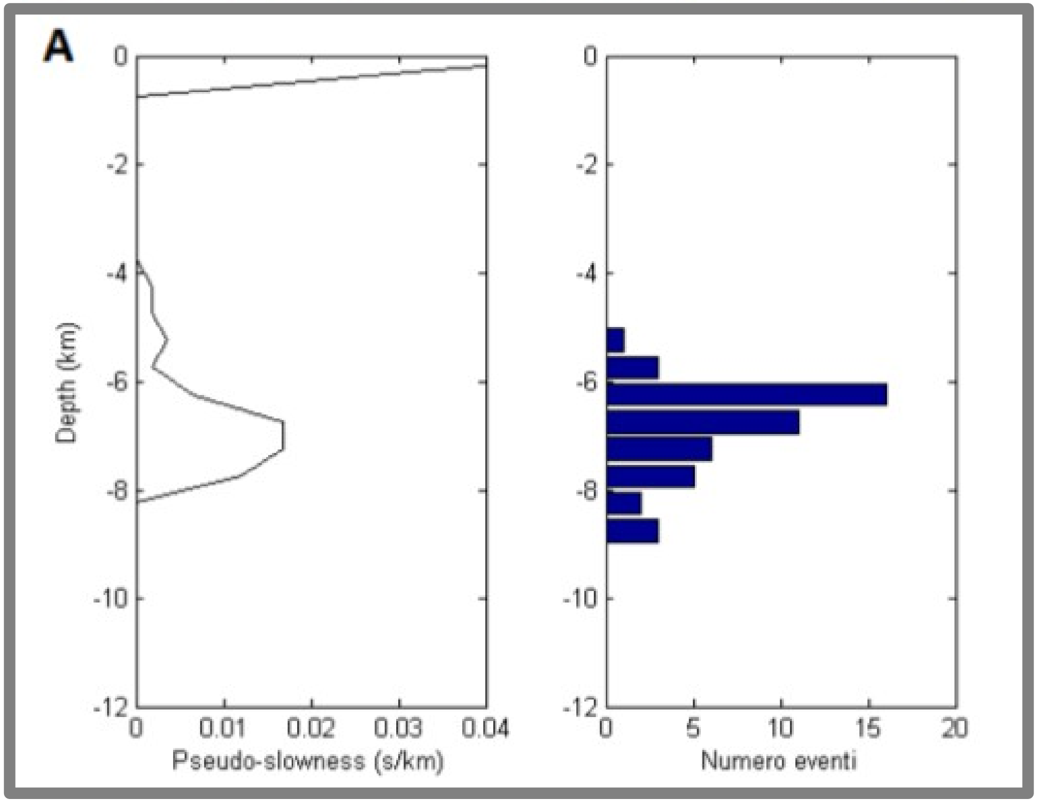

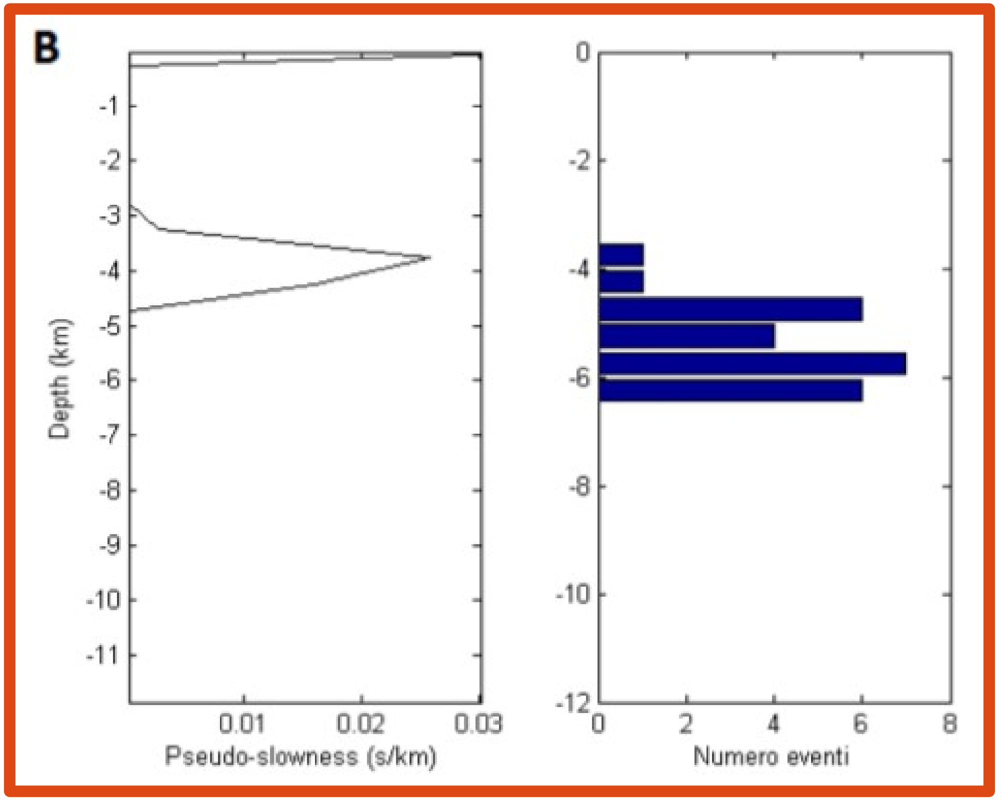

Local earthquake tomography

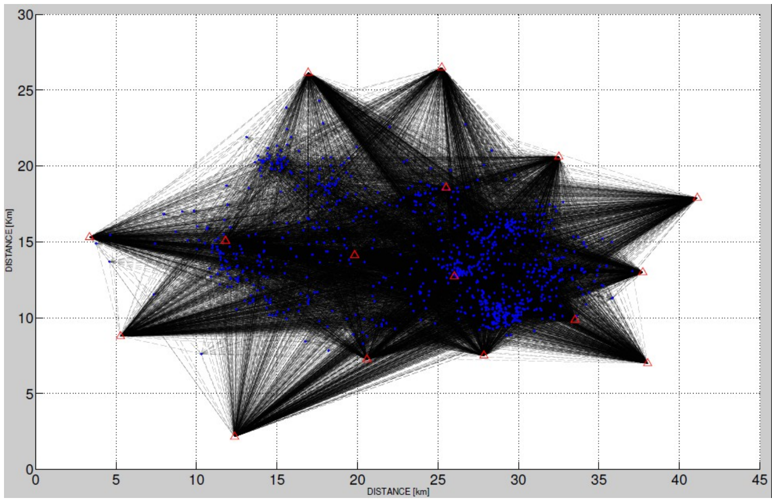

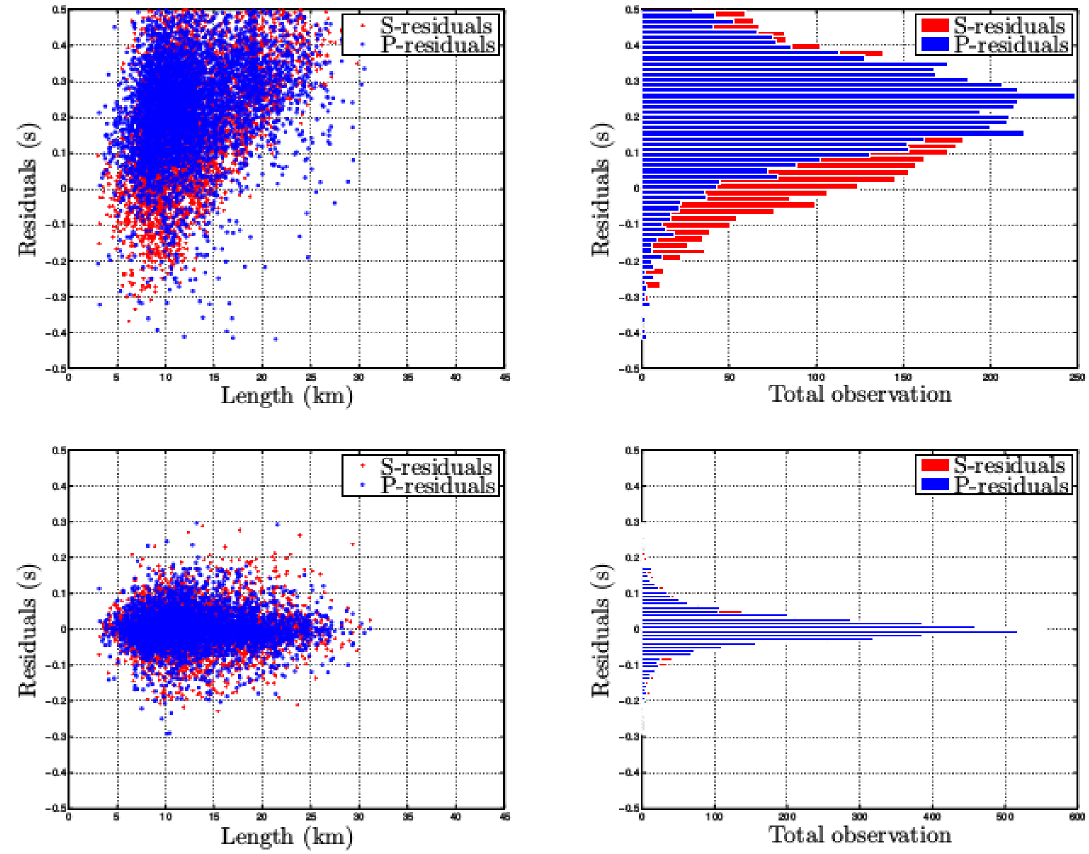

✓~ 900 eqs after filtering for location accuracy and station residuals (- About 4800 P- and 5100 S-waves rays)

✓ Forward Travel-Time calculation: finite-difference solution of the Eikonal equation (Podvin & Lecomte, 1991);

✓ Inversion: The Pstomo package (by Ari Tryggvason), based upon the LSQR conjugate gradient solver.

✓ Separate inversion for P- and S-wave velocities.

Local earthquake tomography: results

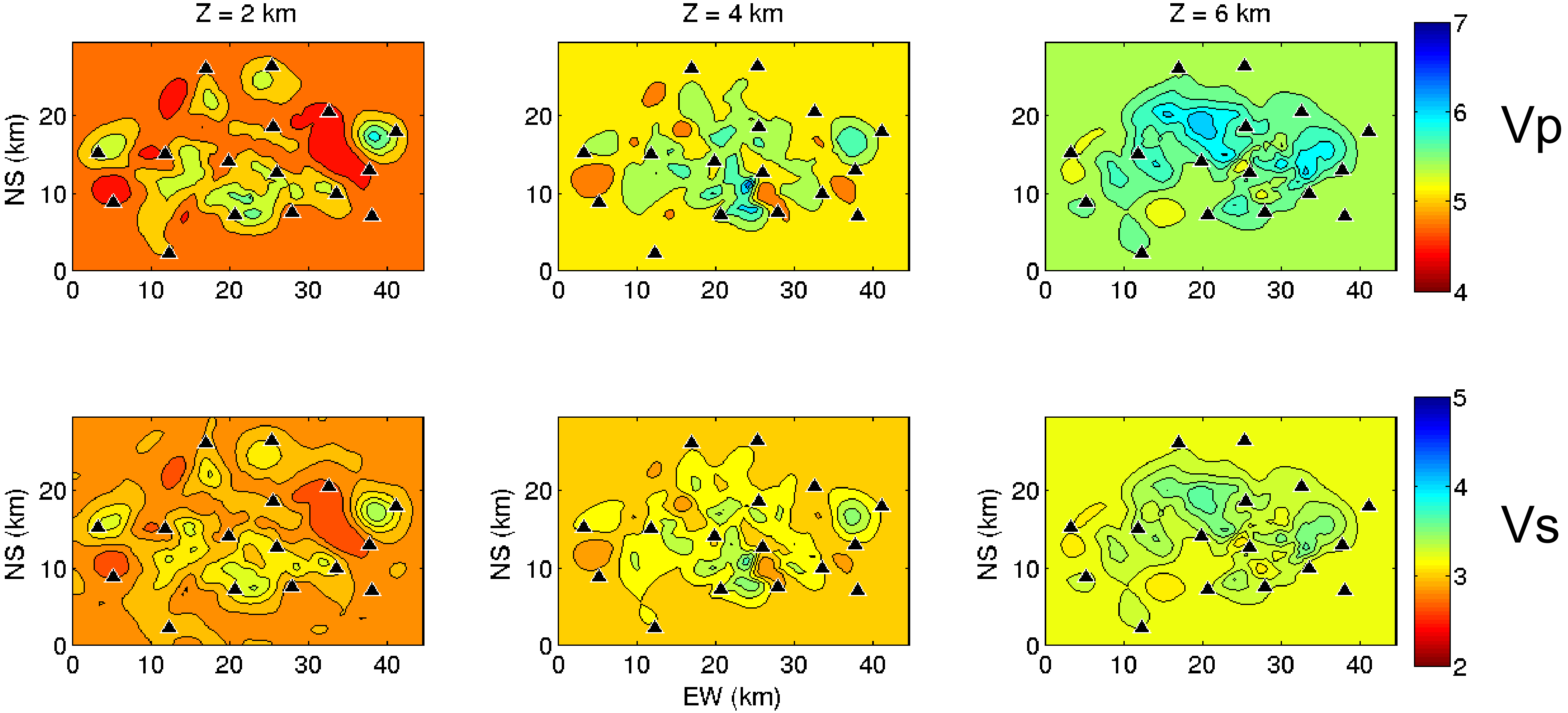

Local earthquake tomography: results

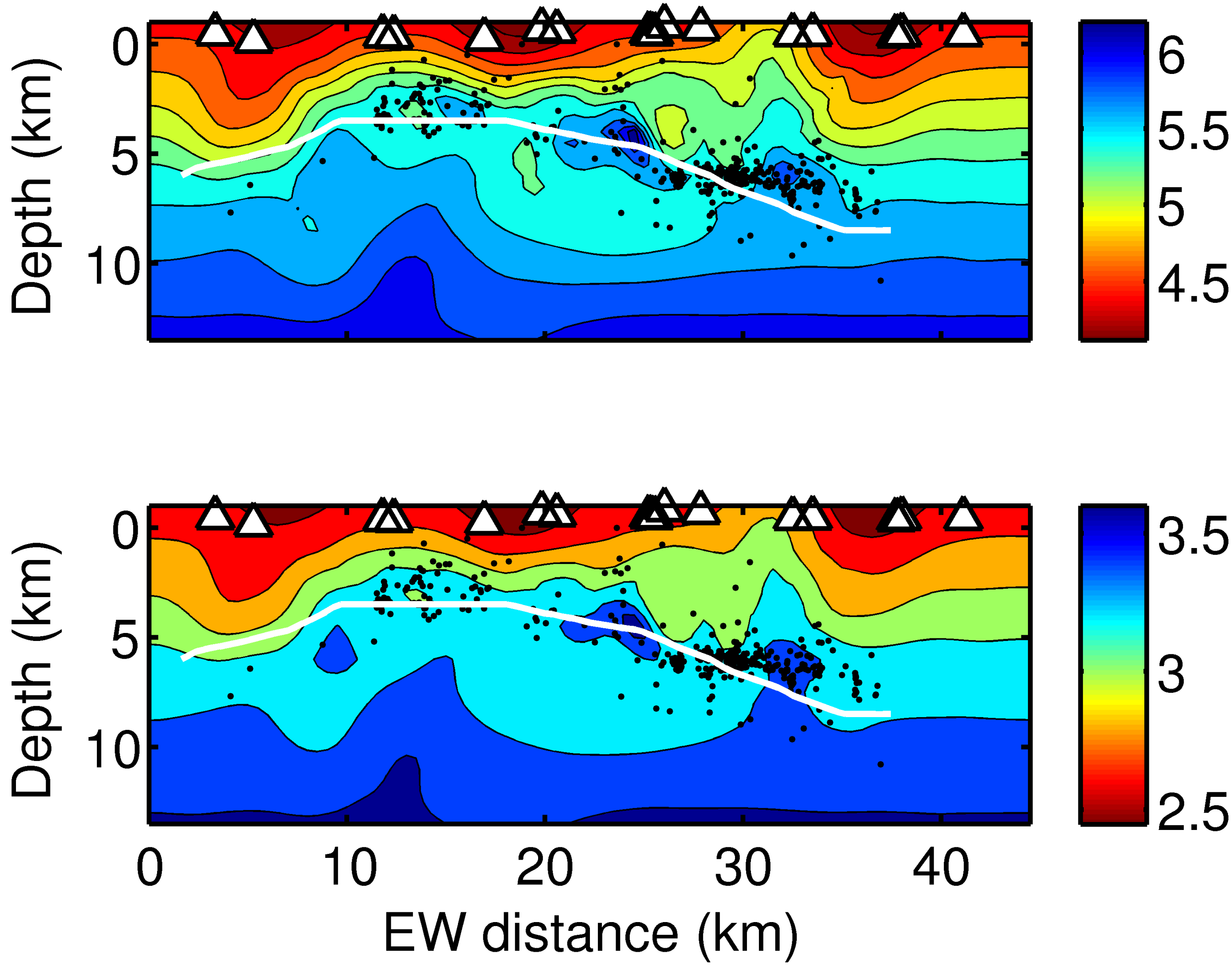

- P- and S-velocity gradients follow the K-marker
- Positive anomalies right above it

Preliminary Interpretation

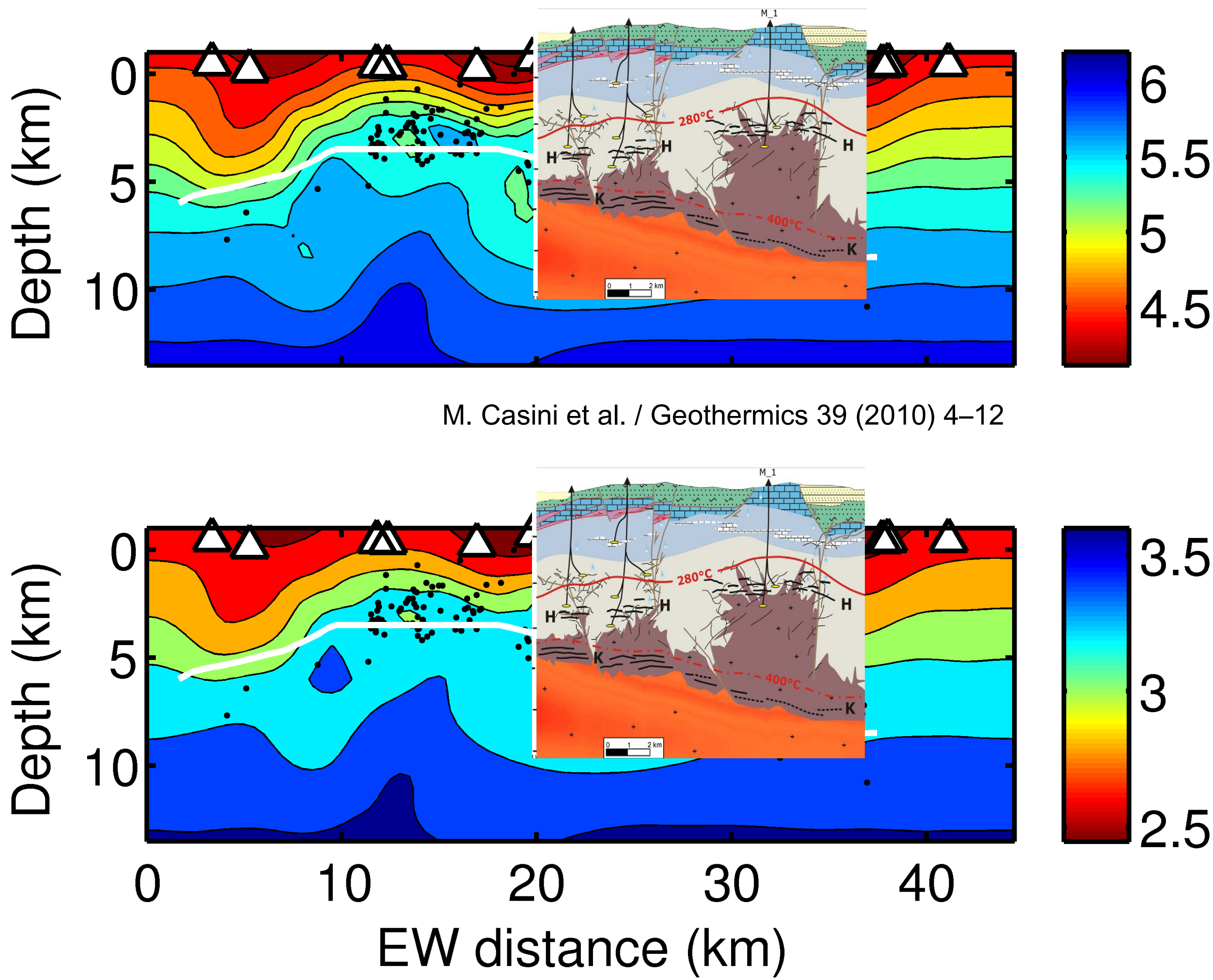

Positive anomalies in correspondence of Pliocene Granitic intrusions
(H marker → target for deep exploitation)

Receiver Function: data-set

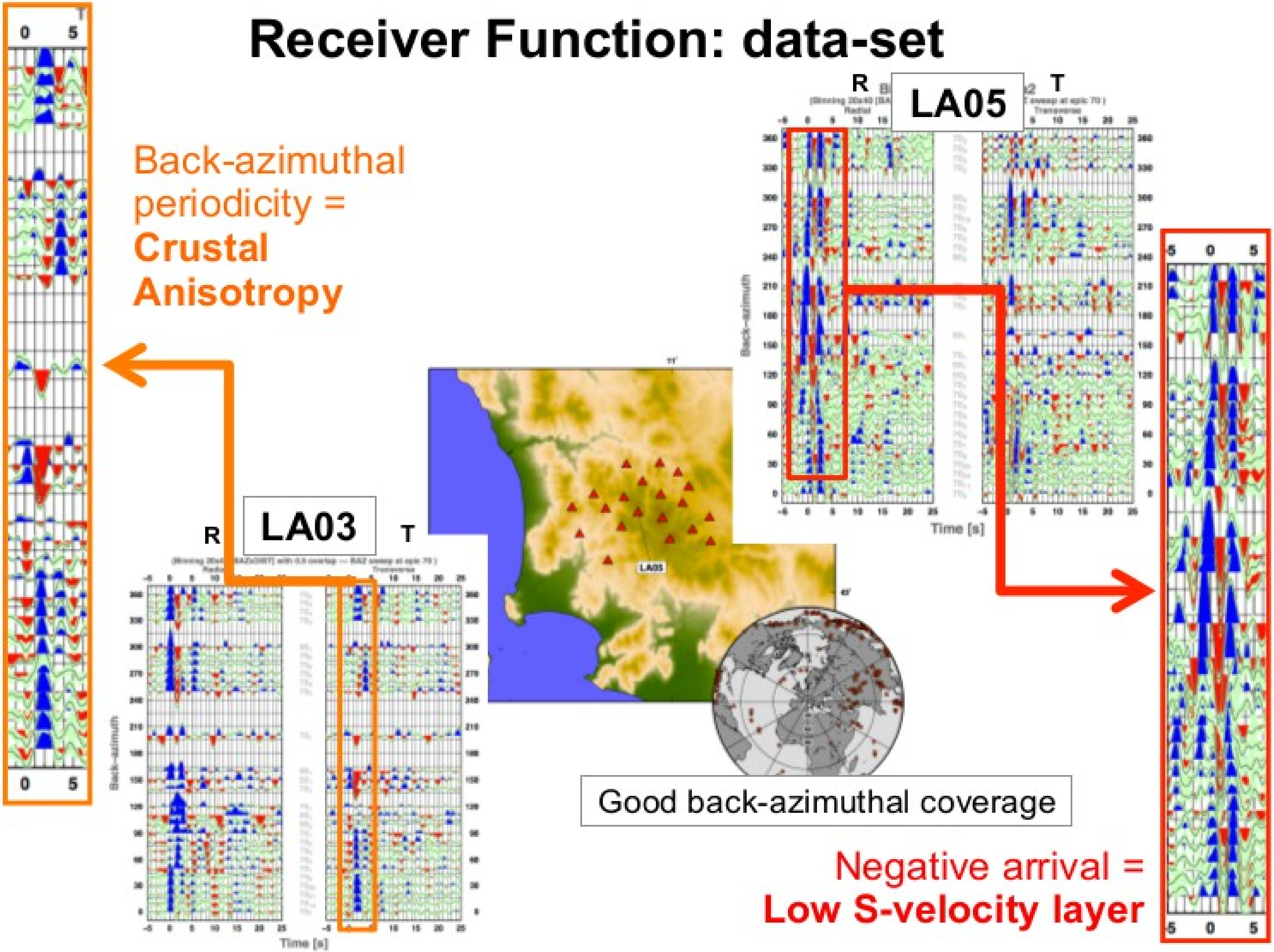

S-wave velocity profiles and depth of anisotropic layers from teleseismic RF

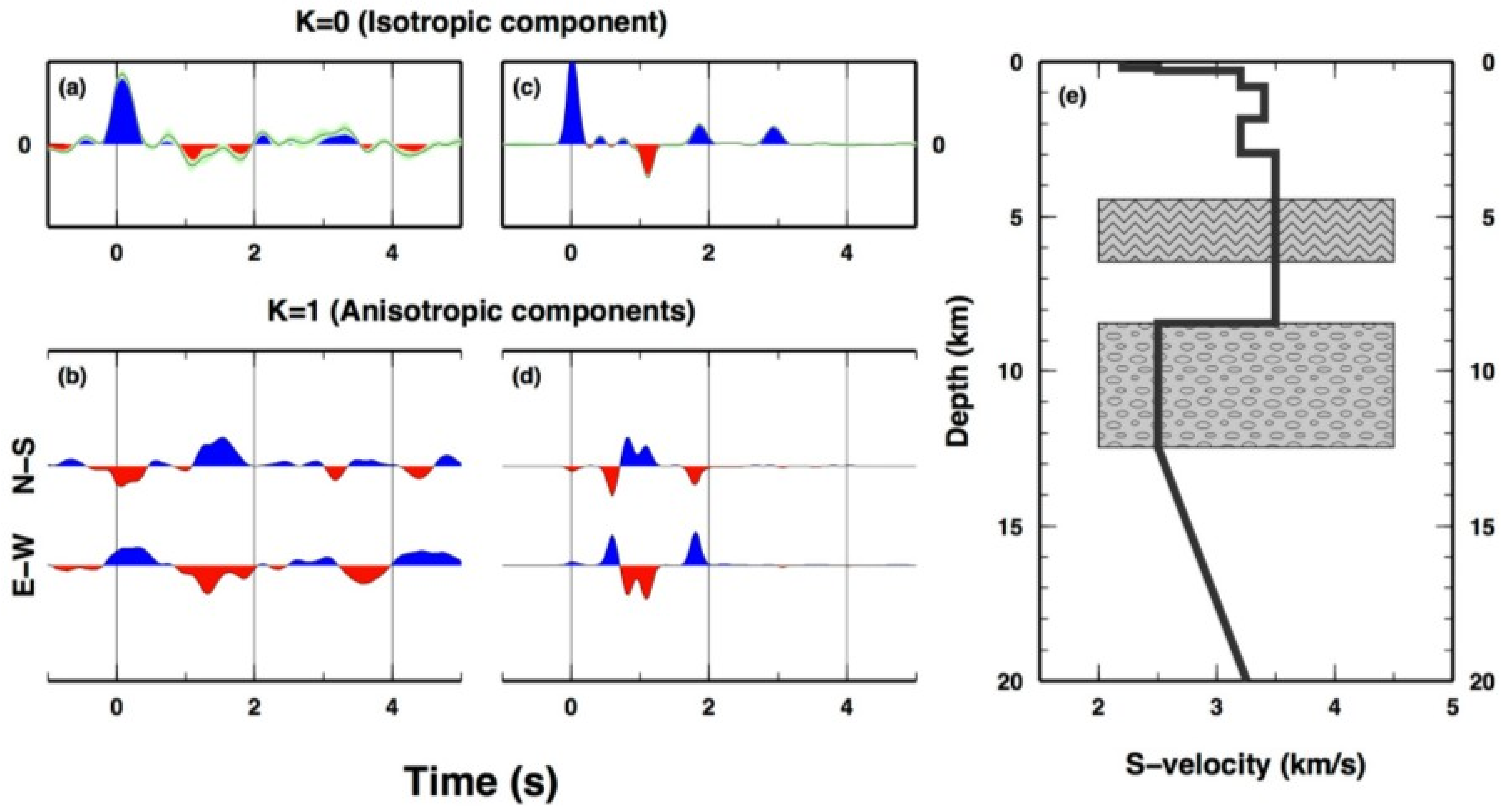

Observed (a,b) and synthetic (c,d) RFs for station LA05. Data are consistent with a P-to-S conversion due to S-velocity discontinuities, and with an anisotropic zones at depth. (e) S-wave velocity profile used to generate the RF in (c-d). Grey-textures indicate the anisotropic zones at depth which generates the conversion recorded on the K=1 coefficients.

Surface wave dispersion from regional quakes

Earthquakes data at regional distances (100-1000 km) are used to derive the dispersion properties of Rayleigh waves, to be inverted for the shallow shear-wave velocity structure.

Example from a Mw=4.0 earthquake at a distance of ~100km

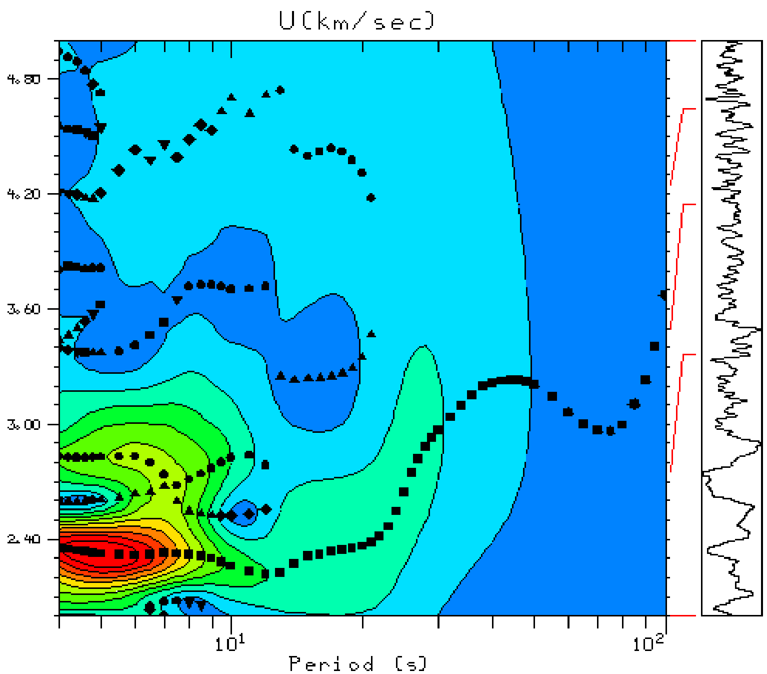

1. Group velocity dispersion for the source-to-receiver path, after Multiple Filtering of single-station recordings.

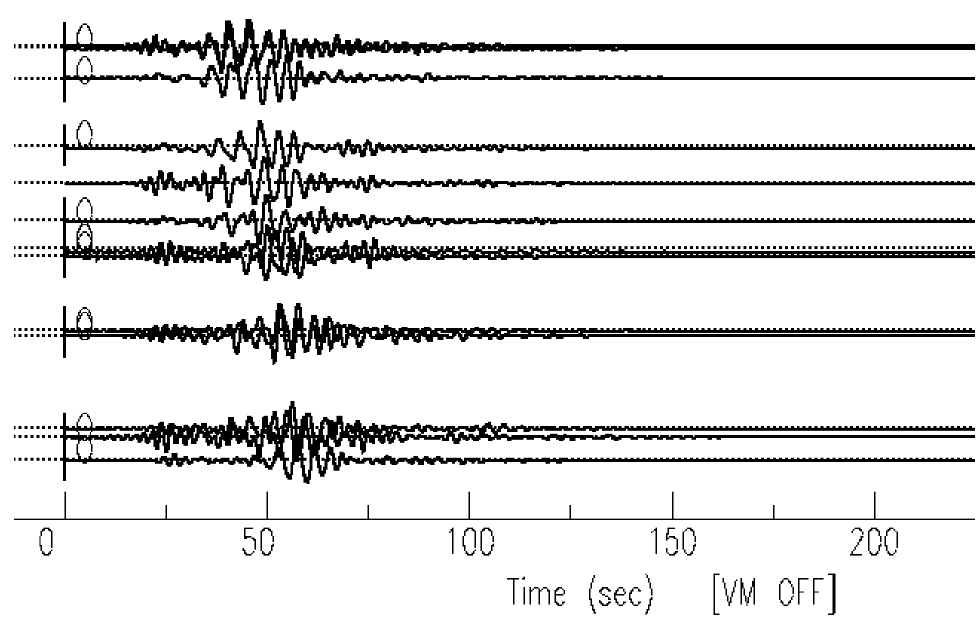

2. Fundamental-mode Rayleigh-wave arrivals after phase-match filtering of multichannel data, following the group dispersion in [1].

S-wave velocity structure from multi-modal inversion of the dispersion curve

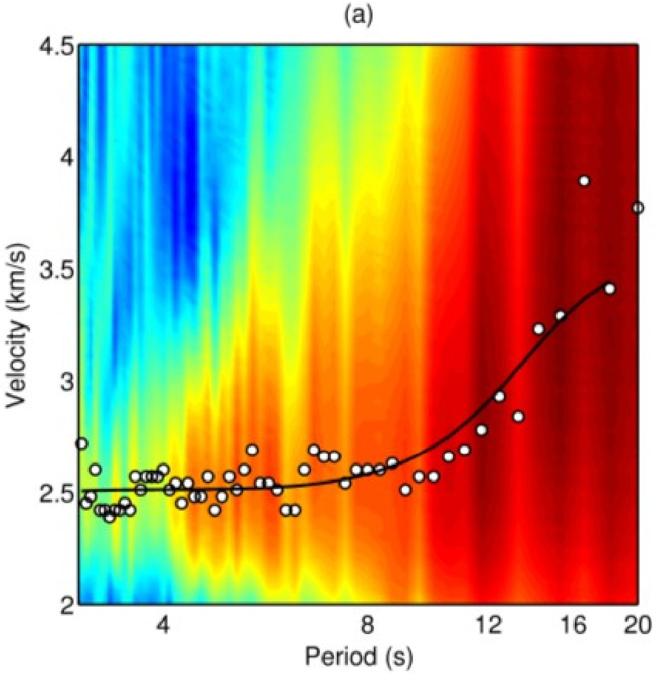

3. p-ω **power spectrum**. Dots indicate the fundamental-mode, phase velocity dispersion curve derived from frequency-slowness analysis of phase-matched filtered data.

We use a misfit function based on the search of the (f,v) points at which the determinant of the propagator matrix attains a **minimum**.

The inversion is conducted using a genetic algorithm iterated on 1000 different starting models, thus allowing for a consistent definition of confidence bounds.

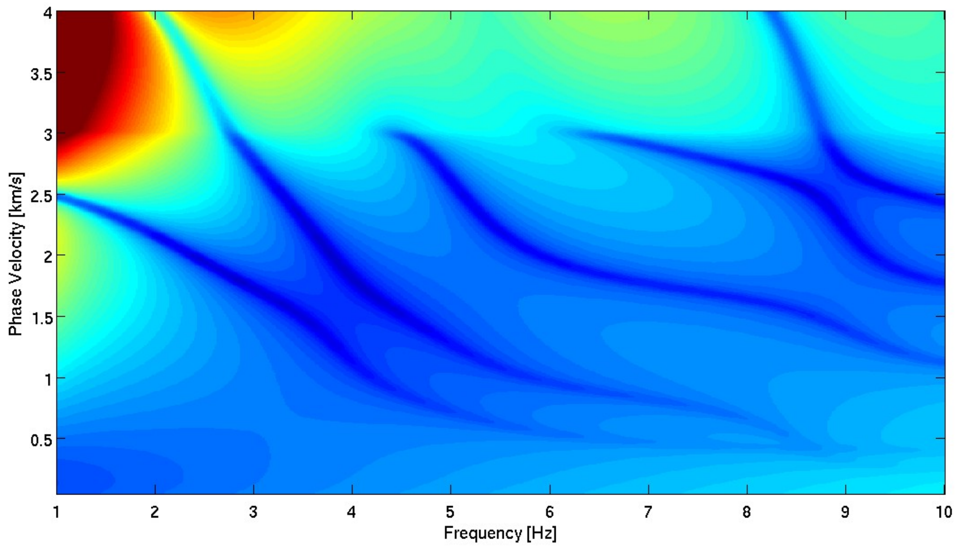

Result of the multi-modal inversion

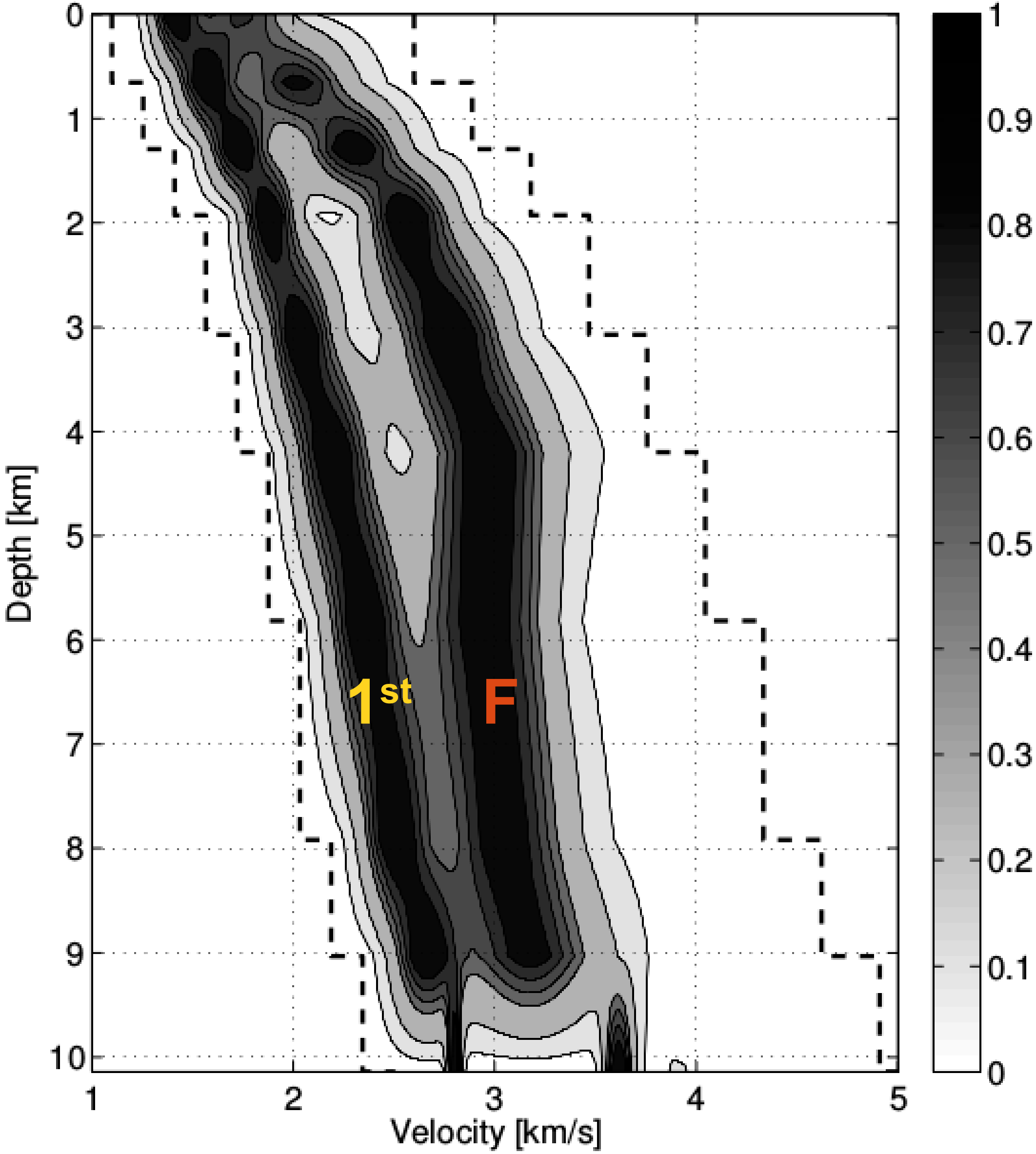

***4. Array-averaged Shear-wave velocity profiles*.**

Results from the inversion indicate two possible velocity profiles, associated with the **fundamental** and **first dispersion mode**. The former is our favorite model.

The 4-8 km depth interval is marked by an extremely weak velocity gradient.

Summary

1. LET has good illumination only for the shallowest 4-5 km. It resolves well the geometry of the different intrusive bodies;

2. Shear-wave splitting of local earthquakes indicates that most of the shallow anisotropy is likely related to the top of the deepest (K-horizon) intrusion;

3. Teleseismic receiver functions indicate (a) low S-wave velocity gradient over the 4-8 km depth range (consistent with 4), and anisotropic layers over the 4-6km and 8-12km depth ranges.

4. Shear-wave velocity profiles from inversion of surface-waves of regional earthquakes indicate a low Vs region spanning the 4-8km depth range.

Though preliminary, these results indicate that the integration of different imaging methods offers a valuable tool for investigating the internal structure of a geothermal field over different scale lengths.

THANKS FOR THE ATTENTION